Progress In Electromagnetics Research, Vol. 134, 543–558, 2013

BLOCK MATRIX PRECONDITIONER METHOD FOR THE ELECTRIC FIELD INTEGRAL EQUATION (EFIE) FORMULATION BASED ON LOOP-STAR BASIS FUNCTIONS

Jae-Hyun Yeom, Huicheol Chin, Hyo-Tae Kim, and Kyung-Tae Kim*

Department of Electrical Engineering, Pohang University of Science and Technology (POSTECH), 77 Cheongam-Ro, Nam-Gu, Pohang, Gyungbuk 790-784, Korea

Abstract—In this paper, electromagnetic scattering problems are analyzed using an electric field integral equation (EFIE) formulation that is based on loop-star basis functions so as to avoid low-frequency instability problems. Moreover, to improve the convergence rate of iterative methods, a block matrix preconditioner (BMP) is applied to the EFIE formulation based on loop star-basis functions. Because the matrix system resulting from the conventional method of moments is a dense matrix, a sparse matrix version of each block matrix is constructed, followed by the inversion of the resultant block sparse matrix using incomplete factorization. Numerical results show that the proposed BMP is efficient in terms of computation time and memory usage.

1. INTRODUCTION

The method of moments (MoM) techniques based on the electric field integral equation (EFIE) formulation have been widely used for analyzing time-harmonic electromagnetic radiation and scattering from conducting surfaces [1–9]. Because the MoM only requires surface discretization of conducting bodies and yields solutions that automatically satisfy the radiation condition, it has some advantages over other numerical methods such as the finite-difference time-domain (FDTD) [10–15] method and the finite element method (FEM) [16–20], particularly in open region problems such as radiation and scattering.

Received 24 September 2012, Accepted 5 December 2012, Scheduled 7 December 2012

* Corresponding author: Kyung-Tae Kim (kkt@postech.ac.kr).

Unfortunately, the MoM based on the EFIE formulation with Rao-Wilton-Glisson (RWG) [21] basis functions is very poorly conditioned at low frequencies. In addition, when the element size is extremely small compared to the wavelength, this problem may also occur. The cause of both cases mentioned above is that the contribution of the vector potential to the resultant matrix becomes negligible, compared to that of the scalar potential. This problem is usually called the low-frequency instability problem. The low-frequency instability problem causes the EFIE with RWG basis functions to be ill-conditioned and the solution to be inaccurate. This low-frequency instability problem has been overcome using loop-star basis functions or loop-tree basis functions in conjunction with frequency scaling of the matrix [3, 22–25]; however, the resultant matrix is also ill-conditioned. When iterative methods, such as the conjugate gradient method (CGM) or the generalized minimal residual method (GMRES) [26, 27], are used to solve the matrix equation, the iterative methods either converges very slowly or diverges. Therefore, it is necessary to find appropriate preconditioning techniques to improve the convergence rate of iterative methods.

In this paper, the block matrix preconditioner (BMP) originally proposed by the FEM community [28, 29] and the MoM for penetrable objects [30] is applied to address the convergence problem in the EFIE formulation based on loop-star basis functions. Furthermore, to compute the BMP efficiently, we first create a sparse matrix from each block matrix by eliminating the small terms in the matrix entries, and then, the inversion of the constructed sparse matrix is approximated using incomplete factorization. Finally, the BMP constructed using the proposed method is compared with the incomplete LU threshold pivoting (ILUTP) preconditioner [31] to demonstrate their performance in terms of memory and computation time, and the effect of the Schur complement, which results from the block matrix decomposition, is investigated when the BMP is constructed.

The remainder of this paper is organized as follows. Section 2 presents a review of the EFIE formulation with loop-star basis functions and presents the proposed preconditioning strategy. Numerical results and conclusions are presented in Section 3 and Section 4, respectively.

2. NUMERICAL METHOD

2.1. EFIE Formulation with Loop-star Basis Functions

When a perfectly conducting object S is placed in free-space, the object is excited by an incident field $\bar{E}^{inc}(\bar{r})$, which induces a surface current $\bar{J}(\bar{r})$ on the surface of the object. The EFIE is derived by enforcing the condition that the total electric field tangential to the object is zero. The EFIE can be written as [1–3]

$$-\hat{n}\times\bar{E}^{inc}(\bar{r})=\hat{n}\times jk\eta\int_{S'}\left(\bar{J}(\bar{r}')G(\bar{r},\bar{r}')+\frac{1}{k^2}\nabla'\cdot\bar{J}(\bar{r}')\nabla G(\bar{r},\bar{r}')\right)dS', \quad (1)$$

where $\hat{n}$ denotes the unit vector normal to the object, $\bar{r}$ and $\bar{r}'$ the position vectors of the observation and source points, respectively, and $\bar{J}(\bar{r}')$ the induced surface current. $G(\bar{r},\bar{r}')$ represents the 3D free-space Green's functions, and k and η are the free-space wave number and impedance, respectively. In addition, in this paper, the time convention used is $e^{j\omega t}$. A set of basis functions $\bar{f}_n$ is used to expand the induced surface current density

$$\bar{J}(\bar{r}')=\sum_{n=1}^{N}a_n\bar{f}_n\left(\bar{r}'\right), \quad (2)$$

where N and a_n are the number of basis functions and the coefficients, respectively, which have yet to be determined. The matrix equation can be constructed by substituting Equation (2) into Equation (1) and testing the integral equation with the same basis function. The resultant matrix equation is

$$\left[Z_1+\frac{1}{k^2}Z_2\right]I=V, \quad (3)$$

where

$$\begin{aligned}
[Z_1]_{m,n} &= \int_S\int_{S'}\bar{f}_m(\bar{r})\cdot\bar{f}_n(\bar{r}')G(\bar{r},\bar{r}')dS'dS,\\
[Z_2]_{m,n} &= -\int_S\int_{S'}\nabla\cdot\bar{f}_m(\bar{r})\nabla'\cdot\bar{f}_n(\bar{r}')G(\bar{r},\bar{r}')dS'dS,\\
[V]_m &= \frac{j}{k\eta}\int_S\bar{f}_m(\bar{r})\cdot\bar{E}^{inc}(\bar{r})dS,
\end{aligned}$$

and I and V are the coefficients of expansion and the discrete form of the excitation, respectively. In Equation (3), the primary cause of the low-frequency instability problem in the MoM approximation can be determined [3, 22–25]. When the frequency approaches zero, the

contribution from Z_2 in Equation (3) dominates that from Z_1 because of the $1/k^2$ term. As a result, the above matrix equation degenerates to $Z_2 I \approx 0$, and Z_2 becomes a nearly singular matrix because $I \neq 0$. This phenomenon makes the resultant matrix equation very difficult to solve at low frequencies. To overcome the low-frequency instability problem, the unknown induced surface current is decomposed into loop currents and star currents [22–25]:

$$\bar{J}(\bar{r}) = \sum_{n=1}^{N_L} a_n^L \bar{f}_n^L(\bar{r}) + \sum_{n=1}^{N_S} a_n^S \bar{f}_n^S(\bar{r}), \tag{4}$$

where N_L and N_S are the number of loop and star basis functions, respectively, and $\bar{f}_n^L(\bar{r})$ and $\bar{f}_n^S(\bar{r})$ correspond to solenoidal parts (loop basis functions) and non-solenoidal parts (star basis functions), respectively. Then, Equation (1) can be converted into the block matrix equation by using loop and star currents as the basis functions and the same testing functions.

The resultant matrix equation is

$$\begin{bmatrix} Z^{LL} & Z^{LS} \\ Z^{SL} & Z^{SS} \end{bmatrix} \begin{bmatrix} I^L \\ I^S \end{bmatrix} = \begin{bmatrix} V^L \\ V^S \end{bmatrix}. \tag{5}$$

The matrix elements in the above equation are given as follows:

$$\left[Z^{LL}\right]_{m,n} = \int_S \int_{S'} \bar{f}_m^L(\bar{r}) \cdot \bar{f}_n^L(\bar{r}') G(\bar{r}, \bar{r}') dS' dS,$$

$$\left[Z^{LS}\right]_{m,n} = \int_S \int_{S'} \bar{f}_m^L(\bar{r}) \cdot \bar{f}_n^S(\bar{r}') G(\bar{r}, \bar{r}') dS' dS,$$

$$\left[Z^{SL}\right]_{m,n} = \int_S \int_{S'} \bar{f}_m^S(\bar{r}) \cdot \bar{f}_n^L(\bar{r}') G(\bar{r}, \bar{r}') dS' dS,$$

$$\left[Z^{SS}\right]_{m,n} = \int_S \int_{S'} \left(\bar{f}_m^S(\bar{r}) \cdot \bar{f}_n^S(\bar{r}') - \frac{1}{k^2} \nabla \cdot \bar{f}_m^S(\bar{r}) \nabla' \cdot \bar{f}_n^S(\bar{r}') \right) G(\bar{r}, \bar{r}') dS' dS,$$

$$\left[V^L\right]_{m,n} = \frac{j}{k\eta} \int_S \bar{f}_m^L(\bar{r}) \cdot \bar{E}^{inc}(\bar{r}) dS,$$

$$\text{and } \left[V^S\right]_m = \frac{j}{k\eta} \int_S \bar{f}_m^S(\bar{r}) \cdot \bar{E}^{inc}(\bar{r}) dS.$$

To obtain a stable system at low frequencies, Equation (5) can be scaled as [3]

$$\begin{bmatrix} 1 & 0 \\ 0 & k \end{bmatrix} \begin{bmatrix} Z^{LL} & Z^{LS} \\ Z^{SL} & Z^{SS} \end{bmatrix} \begin{bmatrix} 1 & 0 \\ 0 & k \end{bmatrix} \begin{bmatrix} 1 & 0 \\ 0 & \frac{1}{k} \end{bmatrix} \begin{bmatrix} I^L \\ I^S \end{bmatrix} = \begin{bmatrix} 1 & 0 \\ 0 & k \end{bmatrix} \begin{bmatrix} V^L \\ V^S \end{bmatrix}. \tag{6}$$

The above equation can be compactly written as

$$\begin{bmatrix} Z^{LL} & kZ^{LS} \\ kZ^{SL} & k^2 Z^{SS} \end{bmatrix} \begin{bmatrix} I^L \\ k^{-1} I^S \end{bmatrix} = \begin{bmatrix} V^L \\ kV^S \end{bmatrix}. \tag{7}$$

The 2×2 block matrix on the left-hand side in Equation (7) is usually called the normalized impedance matrix. Using the above frequency scaling technique and the loop-star basis functions with Equation (7) can yield a stable solution. Unfortunately, when the entries of $Z^{SS}$is evaluated, the charge term arising from divergence of the star basis makes block matrix $k^2 Z^{SS}$ ill-conditioned [3, 23]. As a result, when iterative methods are used to solve Equation (7), it converges very slowly. Therefore, it is essential to use a preconditioner to efficiently solve Equation (7) by iterative methods. In the next section, we introduce a new method for accelerating the convergence of the described iterative methods.

2.2. Proposed Block Matrix Preconditioner

As discussed in the previous section, an effective and novel preconditioner can be incorporated into iterative methods to improve the convergence rate. That is, the preconditioned matrix equation is solved as follows [31]:

$$M^{-1} Z I = M^{-1} V, \tag{8}$$

where M is called the preconditioner, M is a nonsingular matrix of order N. In general, the preconditioner M should be chosen such that the condition number of the preconditioned matrix $M^{-1}Z$ is less than that of the original matrix. As a result, the computation time for iterative methods to solve a matrix equation can be greatly reduced. To avoid low-frequency instability, loop-star basis functions are used to construct Equation (7). Equation (7) resulting from the MoM based on these functions can be partitioned as

$$Z = \begin{bmatrix} Z^{LL} & Z^{LS} \\ Z^{SL} & Z^{SS} \end{bmatrix}. \tag{9}$$

Because block matrices Z^{LL}, Z^{LS}, Z^{SL}, and Z^{SS} in the conventional MoM are dense matrices, sparse versions of these matrices are preferred when computing the inversion of a precondition matrix M^{-1}. Therefore, we use the following approach to construct the sparse matrix. When the matrix system is based on the MoM, the matrix entries corresponding to the self-singularity or near-singularity terms of triangle pairs have strong couplings. Therefore, a sparse matrix corresponding to each dense block matrix is first constructed using those matrix entries that include strong coupling and removing those that have weak coupling. In the previous study, the concept of the diagonal block approximate inverse preconditioner (DBAI) was used to create a sparse matrix from a given dense matrix [24]. In the present study, DBAI is extended to both off-diagonal block matrices

and diagonal block matrices, and is applied to each block matrix with different parameters because each block matrix has the different property. The sparse matrix formulation is given by

$$
\begin{aligned}
Z_{sparse}^{LL} &= \sum_{m=1}^{N} \sum_{n \in S_1(m)}^{N} [Z]_{m,n}, \\
Z_{sparse}^{LS} &= Z_{sparse}^{SL} = \sum_{m=1}^{N} \sum_{n \in S_2(m)}^{N} [Z]_{m,n}, \\
Z_{sparse}^{SS} &= \sum_{m=1}^{N} \sum_{n \in S_3(m)}^{N} [Z]_{m,n}, \\
S_1(m) &= \{\, n \mid \ |\Delta_m - \Delta_n| \ \leq \ N^{0.03}(R_m \ + \ R_n)\}, \\
S_2(m) &= \{\, n \mid \ |\Delta_m - \Delta_n| \ \leq \ N^{0.02}(R_m \ + \ R_n)\}, \\
S_3(m) &= \{\, n \mid \ |\Delta_m - \Delta_n| \ \leq \ N^{0.07}(R_m \ + \ R_n)\},
\end{aligned}
\tag{10}
$$

where N, $S_1(m)$, $S_2(m)$, and $S_3(m)$ denote the number of basis functions, and the three sets of basis functions corresponding to self-singularity or near-singularity of test functions, respectively. $|\Delta_m - \Delta_n|$ is the distance between the centroid of the test triangle and the centroid of the source triangle, including the testing functions and the basis functions, respectively. R_m and R_n represent the radius of the circumcircles of the test triangle and the source triangle, respectively. On the right-hand side of Equation (10), the factors R_m and R_n are introduced to include the entries corresponding to the self-singularity and near-singularity terms in the matrix entries. Furthermore, the weighting coefficients, such as $N^{0.03}$, $N^{0.02}$, and $N^{0.07}$, also allow the sparse matrix to include more entries as N increases [24]. When each weighting coefficient is large, however, the nonzero entries of each block sparse matrix and the computational resources, which are required to construct the preconditioner, also increase dramatically. In order to overcome this problem and deal with the block matrix efficiently, we have chosen the different weighting coefficients. Because the Z^{SS} block matrix is ill-conditioned [23], we have chosen that the sparse matrix corresponding to the Z^{SS} block matrix should include more entries than those corresponding to other block matrices. Thus, the weighting coefficient of $S_3(m)$ is selected to be larger than the other weighting factors in Equation (10), whereas the weighting coefficient corresponding to the off-diagonal block matrices in Equation (9) is least chosen because the off-diagonal block matrices have the weak coupling compared to the Z^{LL} and Z^{SS} block matrices. Since the Z^{LL} block

matrix is well conditioned [23], moreover, the weighting coefficient of $S_1(m)$ is selected to be between the coefficient of Z^{SS} block matrix and that of the off-diagonal block matrices. Once the block sparse matrix is constructed with Equation (10), the BMP can be computed using Gaussian elimination of the block matrix system (9). The 2×2 block matrix can be decomposed into matrix product form [28–30]:

$$\begin{aligned} Z &= \begin{bmatrix} Z^{LL} & Z^{LS} \\ Z^{SL} & Z^{SS} \end{bmatrix} \\ &\approx \begin{bmatrix} Z^{LL}_{sparse} & Z^{LS}_{sparse} \\ Z^{SL}_{sparse} & Z^{SS}_{sparse} \end{bmatrix} \\ &= \begin{bmatrix} I^{LL} & 0 \\ Z^{SL}_{sparse}(Z^{LL}_{sparse})^{-1} & I_{SS} \end{bmatrix} \begin{bmatrix} Z^{LL}_{sparse} & 0 \\ 0 & Z^{SS}_{sparse} - Z^{SL}_{sparse}(Z^{LL}_{sparse})^{-1} Z^{LS}_{sparse} \end{bmatrix} \\ &\quad \begin{bmatrix} I^{LL} & (Z^{LL}_{spasrse})^{-1} Z^{LS}_{sparse} \\ 0 & I^{SS} \end{bmatrix}, \end{aligned} \tag{11}$$

and its inverse can be found as follows:

$$\begin{aligned} Z^{-1} \approx & \begin{bmatrix} I^{LL} & -(Z^{LL}_{sparse})^{-1} Z^{LS}_{sparse} \\ 0 & I^{SS} \end{bmatrix} \\ & \begin{bmatrix} (Z^{LL}_{sparse})^{-1} & 0 \\ 0 & (Z^{SS}_{sparse} - Z^{SL}_{sparse}(Z^{LL}_{sparse})^{-1} Z^{LS}_{sparse})^{-1} \end{bmatrix} \\ & \begin{bmatrix} I^{LL} & 0 \\ -Z^{SL}_{sparse}(Z^{LL}_{sparse})^{-1} & I^{SS} \end{bmatrix}, \end{aligned} \tag{12}$$

where I^{LL} and I^{SS} are the identity matrices of size $N_L \times N_L$ and $N_S \times N_S$, which indicate the number of loop basis functions and star basis functions, respectively. The block matrix in Equation (12) involves inversion of both the first block Z^{LL}_{sparse} and the Schur complement $S = Z^{SS}_{sparse} - Z^{SL}_{sparse}(Z^{LL}_{sparse})^{-1} Z^{LS}_{sparse}$. Because the coupling of $Z^{SL}_{sparse}(Z^{LL}_{sparse})^{-1} Z^{LS}_{sparse}$is negligible, the Schur complement S can be approximated as the inversion of Z^{SS}_{sparse}. The effectiveness of the approximation to Z^{SS}_{sparse} will be considered in the numerical results.

Finally, the proposed BMP M^{-1} can be determined as follows:

$$\begin{aligned} M^{-1} = & \begin{bmatrix} I^{LL} & -(Z^{LL}_{sparse})^{-1} Z^{LS}_{sparse} \\ 0 & I^{SS} \end{bmatrix} \begin{bmatrix} (Z^{LL}_{sparse})^{-1} & 0 \\ 0 & (Z^{SS}_{sparse})^{-1} \end{bmatrix} \\ & \begin{bmatrix} I^{LL} & 0 \\ -Z^{SL}_{sparse}(Z^{LL}_{sparse})^{-1} & I^{SS} \end{bmatrix} \end{aligned} \tag{13}$$

This preconditioner can be applied at each iteration in iterative methods via matrix multiplication. Because the BMP requires the

inversion of each block matrix Z_{sparse}^{LL} and Z_{sparse}^{SS} separately, different dropping parameters can be applied to the approximate inverse methods such as incomplete LU decomposition [31] and the sparse approximate inverse method (SAI) [32, 33]. Moreover, because the Z_{sparse}^{LL} and Z_{sparse}^{SS} block matrices are almost independent of frequency, the BMP has uniform memory demands and construction time over a wide range of frequencies. The effectiveness of the proposed preconditioner will be demonstrated in numerical results.

3. NUMERICAL RESULTS

3.1. Validation of the EFIE Formulation with Loop-star Basis Functions

To validate that EFIE formulation that uses loop-star basis functions, the monostatic radar cross section (RCS) of a perfect electrically conducting (PEC) sphere with a radius of 1 m is analyzed from 10^{-6} Hz to 300 MHz for an x-polarized incident wave impinging on the sphere from the $-z$ direction. The sphere is discretized into 4462 inner edges that have an average length of 0.1λ at 300 MHz. GMRES (50), in conjunction with BMP, is used to solve the matrix system. Here, the notation GMRES (50) implies that GMRES restarts after every 50 iterations. Furthermore, the performance of the BMP is compared with that of the ILUTP precondition [31]. Iteration is terminated once the relative residual error is less than 10^{-3}. From the sparse matrix constructed with Equation (10), the dropping tolerance of the ILUTP is set to 10^{-4} and the approximate inverse of the sub-matrix ($Z_{spasrse}^{LL}$, Z_{sparse}^{SS}) in Equation (13) is also calculated using the ILUTP. The two dropping tolerances of the individual sub-diagonal matrices in the BMP are 10^{-3} and 10^{-6}, respectively. The column pivoting tolerances in the BMP and the ILUTP are 0.05.

Figure 1(a) and Figure 1(b) show the monostatic RCS patterns of a PEC sphere versus frequency. The results obtained from the loop-star basis functions with the BMP and the ILUTP are nearly identical, and they agree with the Mie-series [34, 35] very well over a very wide range of frequencies. Moreover, Figure 1(c) and Figure 1(d) show the number of iterations and CPU time, respectively, that are required for the residual error of GMRES (50) to converge to 10^{-3}. As shown in Figure 1(c) and Figure 1(d), the performance of the BMP is very similar to that of the ILUTP from 10^{-6} Hz to 100 MHz. However, GMRES (50) with the BMP converges faster than GMRES (50) with the ILUTP, especially at frequencies greater than 100 MHz. In Figure 1(e) and Figure 1(f), the construction time and the

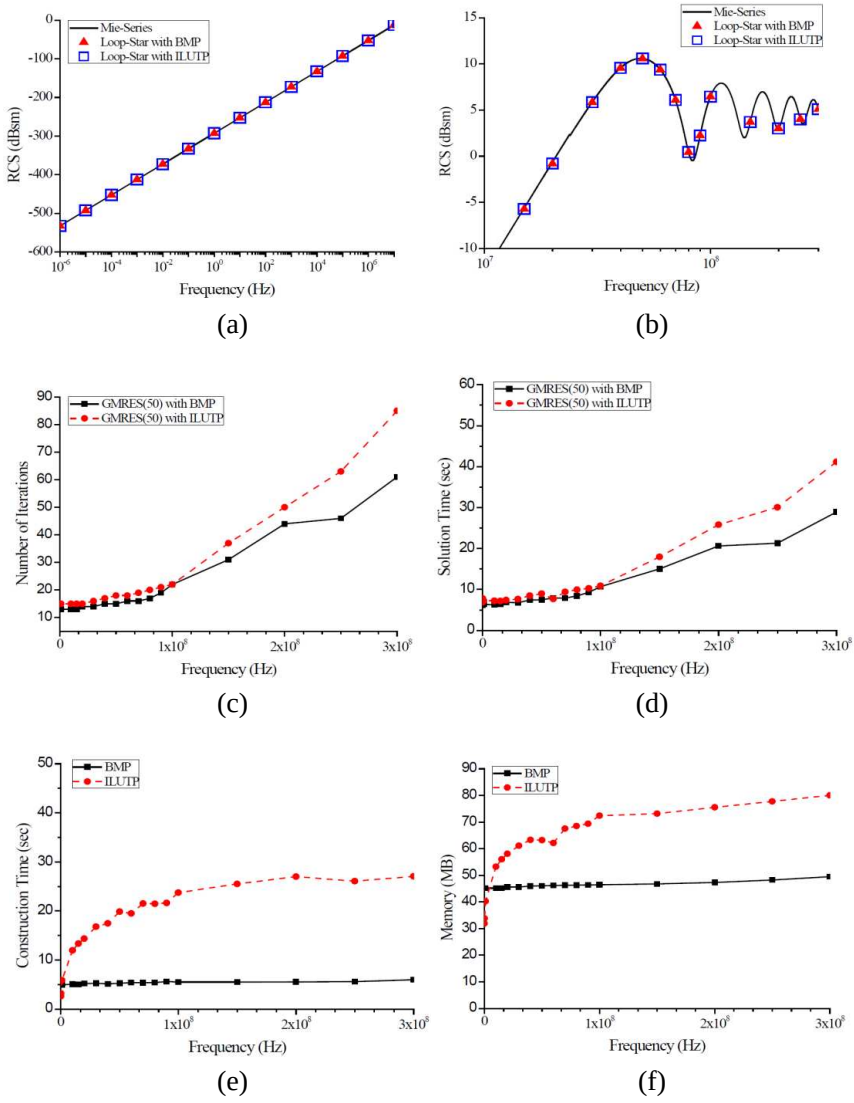

Figure 1. Scattering analysis of a PEC sphere with 1 m radius from 10^{-6} Hz to 300 MHz. (a) Monostatic RCS pattern between 10^{-6} Hz and 10 MHz. (b) Monostatic RCS pattern between 10 MHz and 300 MHz. (c) Number of iterations required to converge to 10^{-3}. (d) CPU time required to solve the matrix system. (e) CPU time required to construct the preconditioner matrix. (f) Memory (MB) required to construct the preconditioner.

memory required for the BMP remains nearly constant from 10^{-6} Hz to 300 MHz. On the other hand, the ILUTP demands significantly more computational resources than BMP as frequency increases.

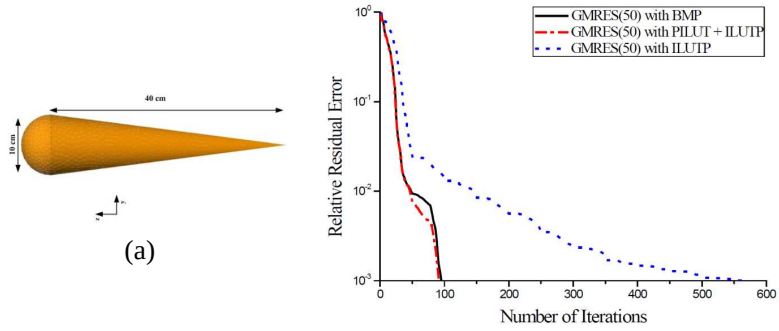

Figure 2. Scattering analysis of a cone-sphere. The total length of the object is 45 cm. A 3 GHz plane wave is incident from the $-z$ direction and is x-polarized. (a) The geometry of a cone-sphere. (b) Convergence history.

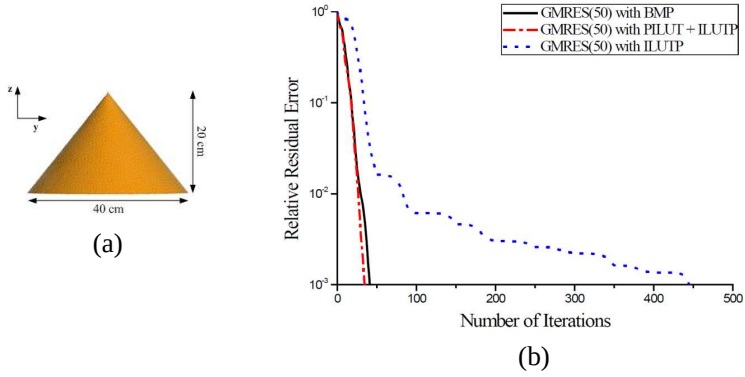

Figure 3. Scattering analysis of an open-cone. The total height of the object is 20 cm; the base radius is 20 cm. A 3 GHz plane wave is incident from the $-z$ direction and is x-polarized. (a) The geometry of an open-cone. (b) Convergence history.

3.2. Convergence Comparison of Iterative Solver with Preconditioner

In this section, the performance of the proposed preconditioner is analyzed for three different objects: a cone-sphere, an open-cone, and an open-cavity. All simulations were conducted with an x-polarized incident wave that impinges upon the object from the $-z$ direction. The cone-sphere and the open-cone were analyzed at 3 GHz, whereas the open-cavity was analyzed at 5 GHz. Moreover, all the objects were discretized with the 0.1λ average edge length. GMRES (50) was also used to solve the matrix equations, and the zero vector was used as the initial value for all simulations. Figures 2–4 show the convergence history when the BMP and the ILUTP are used to solve the matrix system resulting from the use of the MoM. In addition, the dropping tolerance of the ILUTP is set to 10^{-4}, and the approximate inverse of the sub-matrix $(Z^{LL}_{spasrse},\ Z^{SS}_{sparse})$ is calculated using the ILUTP. The two dropping tolerances of the individual sub-diagonal matrices in the BMP also are 10^{-3} and 10^{-6}. In order to show the effect of the Schur complement resulting from the block matrix decomposition, moreover, the partial incomplete LU threshold (PILUT) are used to approximate the inversion of Z^{LL}_{sparse} and construct $Z^{SS}_{sparse} - Z^{SL}_{sparse}(Z^{LL}_{sparse})^{-1}Z^{LS}_{sparse}$ [36]. The ILUTP are also used to approximate the inversion of the Schur complement, resulting from the PILUT. The dropping tolerances of $(Z^{LL}_{sparse})^{-1}$ and $(Z^{SS}_{sparse} - Z^{SL}_{sparse}(Z^{LL}_{sparse})^{-1}Z^{LS}_{sparse})^{-1}$ also are 10^{-3} and 10^{-6}. The

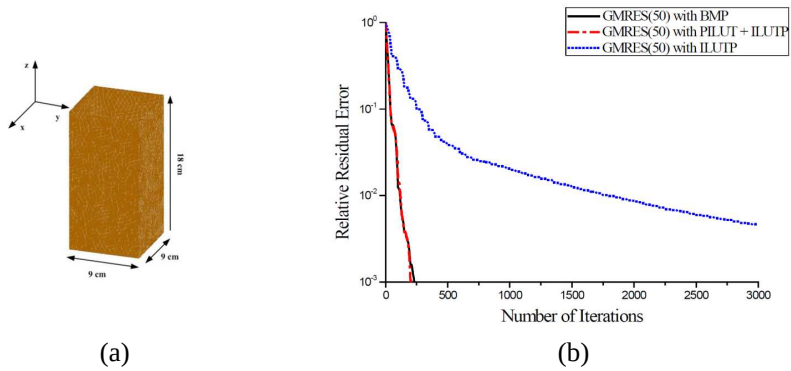

Figure 4. Scattering analysis of an open-cavity. The total height of the object is 18 cm; the width of the object is 9 cm. A 5 GHz plane wave is incident from the $-z$ direction and is x-polarized. (a) The geometry of an open-cavity. (b) Convergence history.

Table 1. Comparisons of the ILUTP-GMRES, BMP-GMRES, PILUT + ILUTP-GMRES for the PEC scattering problems.

	Unknowns (N)	Preconditioning method	Memory (MB)	Iteration (s)	Construction time (s)	Solution time (s)
Cone-sphere	3828 (1277, 2551)	ILUTP ($1e^{-4}$)	51.25	573	10.67	167.34
		BMP ($1e^{-3}$, $1e^{-6}$)	32.07	96	2.1	28.07
		PILUT + ILUTP ($1e^{-3}$, $1e^{-6}$)	75.62	92	32.25	29.83
Open-cone	7915 (2593, 5322)	ILUTP ($1e^{-4}$)	147.25	446	77.81	734.61
		BMP ($1e^{-3}$, $1e^{-6}$)	83.30	41	8.77	65.80
		PILUT + ILUTP ($1e^{-3}$, $1e^{-6}$)	301.91	35	316.03	55.79
Open-cavity	8494 (2811, 5683)	ILUTP ($1e^{-4}$)	200.27	>3000	111.76	>5367.79
		BMP ($1e^{-3}$, $1e^{-6}$)	100.44	234	11.84	395.32
		PILUT + ILUTP ($1e^{-3}$, $1e^{-6}$)	394.80	209	329.89	357.23

column pivoting tolerances of all preconditiong methods are 0.05. Iteration is terminated when the relative residual error is less than 10^{-3}; the maximum number of iterations is limited to 3000. The simulations are carried out on a Pentium 4 with an Intel core i7-2600 processor and 16-GB RAM.

In all simulations, GMRES (50) with the BMP converged considerably faster than GMRES (50) with the ILUTP. In particular, GMRES (50) with the ILUTP preconditioner did not converge in the case of the open-cavity. On the other hand, GMRES (50) with the BMP only required 234 iterations to converge to 10^{-3}. When the BMP is compared to the PILUT + ILUTP, moreover, two results are nearly identical. Here the notation PILUT + ILUTP implies the BMP including the Schur complement. Table 1 summarizes the computational demands of the ILUTP and the BMP for the three objects. In the second column, the number of loop basis functions and star basis functions are included in parenthesis. As shown in Table 1, both the required construction time and the solution time of the BMP are considerably less than those of the ILUTP. Moreover, the BMP requires less memory storage than the ILUTP. When the BMP is compared to the BMP including the Schur complement, the proposed BMP is efficient in terms of computation time and memory usage.

4. CONCLUSION

Electromagnetic scattering problems are analyzed using EFIE formulation based on loop-star basis functions. Use of an EFIE formulation using loop-star basis functions remedies the low- frequency instability that occurs in RWG basis functions. However, the matrix resulting from the EFIE formulation using loop-star basis functions is not suitable for use with iterative methods because of its requirement for a large number of iterations. In this paper, we propose a new method for improving the convergence rate of iterative methods and computing a preconditioner efficiently. To construct a block sparse matrix from a dense matrix, the matrix entries including strong coupling are the only ones retained, and GMRES with the BMP is applied to solve EFIE formulation based on loop-star basis functions. As a result, the preconditioned EFIE using the proposed BMP dramatically reduced the number of iterations required for convergence. Through numerical results, the proposed BMP is efficient in terms of computation time and memory usage.

ACKNOWLEDGMENT

This work was supported by the Brain Korea 21 (BK 21) Project in 2012.

REFERENCES

1. Harrington, R. F., *Field Computation by Moment Methods*, Macmillan, 1968.
2. Gibson, W. C., *The Method of Moments in Electromagnetics*, Chapman & Hall/CRC, 2007.
3. Chew, W. C., M. S. Tong, and B. Hu, *Integral Equation Methods for Electromagnetic and Elastic Waves*, Morgan & Claypool, 2008.
4. Wang, W. and N. Nishimura, "Calculation of shape derivatives with periodic fast multipole method with application to shape optimization of metamaterials," *Progress In Electromagnetic Research*, Vol. 127, 46–64, 2012.
5. Liu, Z.-L. and J. Yang, "Analysis of electromagnetic scattering with higher order moment method and NURBS model," *Progress In Electromagnetic Research*, Vol. 96, 83–100, 2009.
6. Wang, A.-Q., L.-X. Guo, Y.-W. Wei, and J. Ma, "Higher order method of moments for bistatic scattering from 2D PEC rough

surface with geometric modeling by NURBS surface," *Progress In Electromagnetic Research*, Vol. 130, 85–104, 2012.

7. Liu, Z. H., E. K. Chua, and K. Y. See, "Accurate and efficient evaluation of method of moments matrix based on a generalized analytical approach," *Progress In Electromagnetic Research*, Vol. 94, 367–382, 2009.
8. Ubeda, E., J. M. Tamayo, and J. M. Rius, "Taylor-orthogonal basis functions for the discretization in method of moments of second kind integral equations in the scattering analysis of perfectly conducting or dielectric objects," *Progress In Electromagnetic Research*, Vol. 119, 85–105, 2011.
9. Guo, L.-X., A.-Q. Wang, and J. Ma, "Study on EM scattering from 2-D target above 1-D large scale rough surface with low grazing incidence by parallel MoM based on PC clusters," *Progress In Electromagnetic Research*, Vol. 89, 149–166, 2009.
10. Taflov, A. and S. C. Hagness, *Computational Electrodynamics: The Finite-difference Time-domain Method*, Artech House, 2000.
11. Wang, J. B., B. H. Zhou, L. H. Shi, C. Gao, and B. Chen, "A novel 3D weakly conditionally stable FDTD algorithm," *Progress In Electromagnetic Research*, Vol. 130, 525–540, 2012.
12. Xiong, R., B. Chen, Y. Mao, B. Li, and Q.-F. Jing, "A simple local approximation FDTD model of short apertures with a finite thickness," *Progress In Electromagnetics Research*, Vol. 131, 153–167, 2012.
13. Chen, C.-Y., Q. Wu, X.-J. Bi, Y.-M. Wu, and L. W. Li, "Characteristic analysis for FDTD based on frequency response," *Journal of Electromagnetic Waves and Applications*, Vol. 24, Nos. 2–3, 283–292, 2010.
14. Sirenko, K., V. Pazynin, Y. K. Sirenko, and H. Bagci, "An FFT-accelerated FDTD scheme with exact absorbing conditions for characterizing axially symmetric resonant structures," *Progress In Electromagnetics Research*, Vol. 111, 331–364, 2011.
15. Kusiek, A. and J. Mazur, "Analysis of scattering from arbitrary configuration of cylindrical objects using hybrid finite-difference mode-matching method," *Progress In Electromagnetics Research*, Vol. 97, 105–127, 2009.
16. Jin, J. M., *The Finite Element Method in Electromagnetics*, Wiley, 2002.
17. Ping, X. W. and T.-J. Cui, "The factorized sparse approximate inverse preconditioned conjugate gradient algorithm for finite element analysis of scattering problems," *Progress In Electromag-*

netics Research, Vol. 98, 15–31, 2009.

18. Fotyga, G., K. Nyka, and M. Mrozowski, "Efficient model order reduction for FEM analysis of waveguide structures and resonators," *Progress In Electromagnetic Research*, Vol. 127, 259–275, 2012.
19. Tian, J., Z.-Q. Lv, X.-W. Shi, L. Xu, and F. Wei, "An efficient approach for multifrontal algorithm to solve non-positive definite finite element equations in electromagnetic problems," *Progress In Electromagnetics Research*, Vol. 95, 121–133, 2009.
20. Gomez-Revuelto, I., L. E. Garcia-Castillo, and M. Salazar-Palma, "Goal-oriented self-adaptive HP-strategies for finite element analysis of electromagnetic scattering and radiation problems," *Progress In Electromagnetics Research*, Vol. 125, 459–482, 2012.
21. Rao, S. M., D. R. Wilton, and A. W. Glisson, "Electromagnetic scattering by surfaces of arbitrary shape," *IEEE Transactions on Antenna and Propagation*, Vol. 30, 409–418, 1982.
22. Giuseppe Vecchi, G., "Loop-star decomposition of basis functions in the discretization of the EFIE," *IEEE Transaction on Antenna and Propagation*, Vol. 47, No. 2, 339–346, 1999.
23. Zhao, J. S. and W. C. Chew, "Integral equation solution of Maxwell's equations from zero frequency to microwave frequencies," *IEEE Transactions on Antenna and Propagation*, Vol. 48, 1635–1645, 2000.
24. Lee, J. F., R. Lee, and R. J. Burkholder, "Loop star basis functions and a robust preconditioner for EFIE scattering problems," *IEEE Transactions on Antenna and Propagation*, Vol. 51, No. 8. 1855–1863, 2003.
25. Eibert, T. F., "Iterative-solver convergence for loop-star and loop-tree decompositions in method of moments solutions of the electric-field integral equation," *IEEE Antenna and Propagation Magazine*, Vol. 46, No. 3, 2004.
26. Hestenes, M. R. and E. Steilfel, "Method of conjugate gradients for solving linear systems," *Journal of Research of the National Bureau of Standards*, Vol. 49, 409–436, 1952.
27. Saad, Y., "GMRES: A generalized minimal residual algorithm for solving nonsymmetric linear systems," *SIAM Journal on Scientific and Statistical Computing*, Vol. 7, 856–869, 1986.
28. Lee, J. F. and D. K. Sun, "p-type multiplicative Schwarz (pMUS) method with vector finite elements for modeling three-dimensional waveguide discontinuities," *IEEE Transactions on Microwave Theory and Technology*, Vol. 52, No. 3, 864–870, 2004.

29. Lee, J. F., R. Lee, and F. Teixeira, "Hierarchical vector finite elements with p-type non-overlapping Schwarz method for modeling waveguide discontinuities," *CEMS — Computer Modeling in Engineering & Sciences*, Vol. 5, No. 5, 423–434, 2004.
30. Malas, T. and L. Gurel, "Schur complement preconditioners for surface integral equation formulation of dielectric problems solved with the multilevel fast multipole algorithm," *SIAM Journal on Scientific Computing*, Vol. 33, No. 5, 2440–2467, 2011.
31. Saad, Y., *Iterative Methods for Sparse Linear Systems*, 2nd Edition, PWS, 2003.
32. Benzi, M., C. D. Meyer, and M. Tuma, "A sparse approximate inverse preconditioner for the conjugate gradient method," *SIAM Journal on Scientific and Statistical Computing*, Vol. 17, 1135–1149, 1996.
33. Benzi, M., "A sparse approximate inverse preconditioner for nonsymmetric linear systems," *SIAM Journal on Scientific and Statistical Computing*, Vol. 19, 968–994, 1998.
34. Balanis, C. A., *Advanced Engineering Electromagnetics*, Wiley, New York, 1989.
35. Jin, J. M., *Theory and Computation of Electromagnetic Fields*, Wiley, 2010.
36. Li, N., B. Suchomel, D. O. Kuffuor, R. Li, and Y. Saad, "ZITSOL: Iterative solvers package version 1.0," Department of Computer Science and Engineering, University of Minnesota, Minneapolis MN55455, 2010, http://www-user.cs.umn.edu/∼saad/software/.